

## EFFECT OF RAIL GRINDING CONDITIONS ON SUB-SURFACE MICROSTRUCTURE AND SURFACE ROUGHNESS OF FATIGUED RAILS<sup>1</sup>

Diego Zapata<sup>2</sup>  
Juan Felipe Santa<sup>3</sup>  
J.C Sánchez<sup>4</sup>  
J.C González<sup>5</sup>  
Alejandro Toro<sup>6</sup>

### Abstract

Rail grinding is a common practice in railroad industry to maintain the profile and remove wear marks (fatigue cracks, head checks, etc) from the rail's surface. This practice changes both the sub-surface microstructure and the surface roughness and affects the wear performance of the rail. In this work, the effect of rail grinding on sub-surface rail microstructure and surface roughness was evaluated and correlated with rail's wear performance in the field. The grinding tests were carried out in a low density traffic line of a commercial railroad, with the aid of a rail-grinder car equipped with eight grinding wheels. The tests were done by using the same grit-size, two linear velocities and two loads applied under dry conditions. In order to ensure uniformity of the initial properties, the tested rails had the same tonnage history. The fatigued rails were inspected before the test and the defects were properly identified and quantified. The ground specimens were cut to evaluate the microstructure, micro-hardness profile and roughness after each grinding condition. The analysis of the microstructure of tested specimens revealed the formation of a highly deformed, hard layer with thickness between 10 and 20  $\mu\text{m}$ . Relationships among rail-grinder car velocity, load between rail and grit and roughness of the rails were established. The results indicated that higher loads lead to higher roughness with Ra ranging from 1 to 5  $\mu\text{m}$  in the fatigued zone. These roughness values are very low when compared to the international standards, which is believed to delay the initiation of fatigue cracks. New rail grinding conditions were suggested which could lead to a more effective removal of cracks on the surface.

**Keywords:** Rolling contact fatigue; Rail grinding; Head checks.

### EFEITO DAS CONDIÇÕES DE ESMERILHADO NA MICROESTRUTURA E INTEGRIDADE SUPERFICIAL DE TRILHOS FADIGADOS

#### Resumo

O Esmerilhado de trilhos é uma prática comum na indústria de transporte ferroviário para manter o perfil e para retirar as marcas de desgaste (trincas de fadiga) das superfícies. Esta prática altera a microestrutura da sub-superfície e a rugosidade da superfície, ao mesmo tempo que muda o desempenho em desgaste do trilho. Neste trabalho, o efeito das variáveis do esmerilhado na microestrutura e na rugosidade superficial dos trilhos foi avaliada e correlacionada com as variáveis de operação. Os ensaios foram feitos numa linha de baixa densidade de tráfego com a ajuda de um máquina esmerilhadora ferroviária equipada com oito rebolos. Os testes foram feitos usando o mesmo tamanho de grão, duas velocidades lineares e duas cargas aplicadas em condições secas. A fim de assegurar a uniformidade de propriedades iniciais, as amostras foram selecionadas de trilhos com o mesmo histórico de carregamento. Os trilhos foram inspecionados antes do ensaio e os defeitos foram quantificados. As amostras foram cortadas para avaliar a microestrutura, o perfil de micro-dureza e a rugosidade após cada condição de esmerilhado. A análise da microestrutura da sub-superfície das amostras revelou a presença de uma camada dura de 10 à 20  $\mu\text{m}$  de espessura. Após os ensaios foram estabelecidas relações entre a velocidade do carro da esmerilhadora, a carga aplicada e a rugosidade superficial dos trilhos. Os resultados indicaram que as cargas mais elevadas levam ao aumento da rugosidade, cujo valor de Ra variou entre 1 e 5  $\mu\text{m}$  na zona o contato. Esses valores são muito baixos em comparação com os padrões internacionais, o que atrasa o início de trincas de fadiga. Novas condições de esmerilhado foram sugeridas, com o intuito de facilitar uma remoção mais eficaz de trincas na superfície.

**Palavras chave:** Fadiga de contato; Esmerilhado de trilhos; Trincas de fadiga.

<sup>1</sup> Technical contribution to the First International Brazilian Conference on Tribology – TribobR-2010, November, 24<sup>th</sup>-26<sup>th</sup>, 2010, Rio de Janeiro, RJ, Brazil.

<sup>2</sup> M.Sc., National University of Colombia. Tribology and Surfaces Group. [dazapata@unal.edu.co](mailto:dazapata@unal.edu.co)

<sup>3</sup> M.Sc., National University of Colombia. Tribology and Surfaces Group. [jfsanta@unal.edu.co](mailto:jfsanta@unal.edu.co),

<sup>4</sup> M.Sc., National University of Colombia. Tribology and Surfaces Group. [jcsanchezo@unal.edu.co](mailto:jcsanchezo@unal.edu.co),

<sup>5</sup> M.E. National University of Colombia. Tribology and Surfaces Group. [jcgonzalv@unal.edu.co](mailto:jcgonzalv@unal.edu.co),

<sup>6</sup> Ph.D. National University of Colombia. Tribology and Surfaces Group. [atoro@unal.edu.co](mailto:atoro@unal.edu.co),

## 1 INTRODUCTION

Rail grinding has been performed in commercial railways since the 1980's to remove surface defects such as head checks and corrugations, as well as to preserve the rail's profile. Rail grinding is currently carried out by trains equipped with rotating grinding wheels driven by electric motors; the rail's roughness after grinding depends on the characteristics and condition of the abrasive wheels, the applied pressure and the speed and angle between the grinding stones and the rail. Kapoor et al.<sup>(1)</sup> showed that the surface roughness has a significant effect on how loads are transmitted at the contact interface between rail and wheel since it causes high local pressures at the contacting roughness peaks.

In agreement with Kapoor's results, Bucher and Knothe<sup>(2)</sup> showed that roughness parameters have a strong influence on the gradient of the linear region of the creep-force curve. Also, Chen, Ishida and Nakahara<sup>(3)</sup> analyzed the influence of roughness orientation on asperity contact pressure and the adhesion coefficient.

Baek, Kyogoku and Nakahara<sup>(4)</sup> found that the variations of traction coefficient could be associated to both surface roughness and hardness changes in service. Satoh and Iwafuchi<sup>(5)</sup> studied the effect of rail grinding conditions on the sub-surface microstructure in fatigued rails by means of metallographic observation and concluded that, if carried out properly, rail grinding allows maintaining the rolling contact fatigue damage within acceptable limits.

In this work, the effect of rail grinding conditions on rail roughness and sub-surface microstructure was studied in order to develop new rail grinding procedures to improve resistance to Rolling Contact Fatigue (RCF). The rail grinding tests were performed using the same grit-size, two linear velocities and two loads applied under dry condition. Relations between rail grinding velocity, load between rail and grit and roughness surface parameters were established.

## 2 EXPERIMENTAL PROCEDURE

### 2.1 Inspection of Fatigue Rails

Fatigued R260-type rail samples were extracted from a 200 m radius curve of a commercial line. The surfaces were inspected in a *Nikon* stereoscope and a Scanning Electron Microscope (SEM) *JEOL* 5910LV and after that, the rail samples were cut to evaluate the depth, length and angle of the cracks found. Based on the analysis of the results, rail grinding procedures were designed to properly remove the affected material from the rails' surface.

### 2.2 Rail Grinding Tests

The grinding procedures were performed in a low density traffic line using a *Harsco Track Technologies* TG8 rail grinding machine. The samples were sections of rails extracted from a commercial line, which were placed in the low density traffic line using clamps. The grinding machine has 8 heads (4 on each rail) and several grinding patterns can be selected. Each grinding wheel can be adjusted to an attack angle between +45° and -40° (see Figure 1 for details) and the travel velocity can be varied between 1.6 and 13 km/h. Three rail grinding procedures were developed using different velocities and pressures applied to the rail, as shown in Table 1.

Photographs were taken at the beginning of the test to study the changes introduced by the grinding operation.

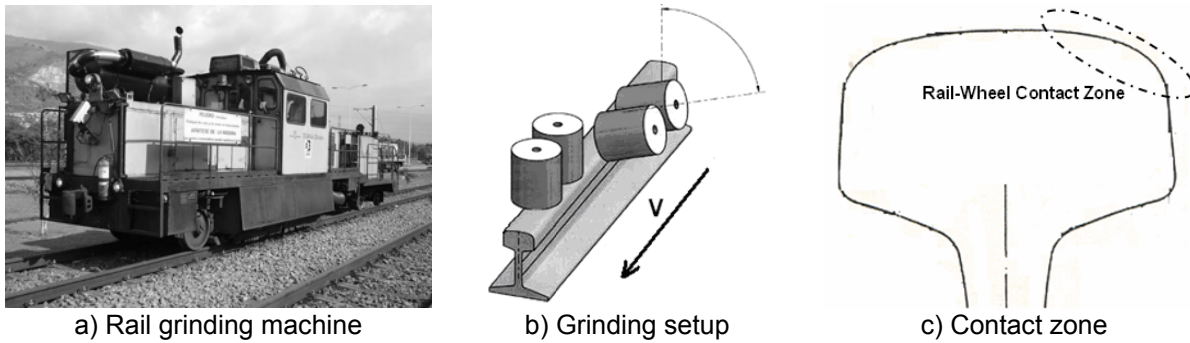


**Figure 1.** Details of grinding operation

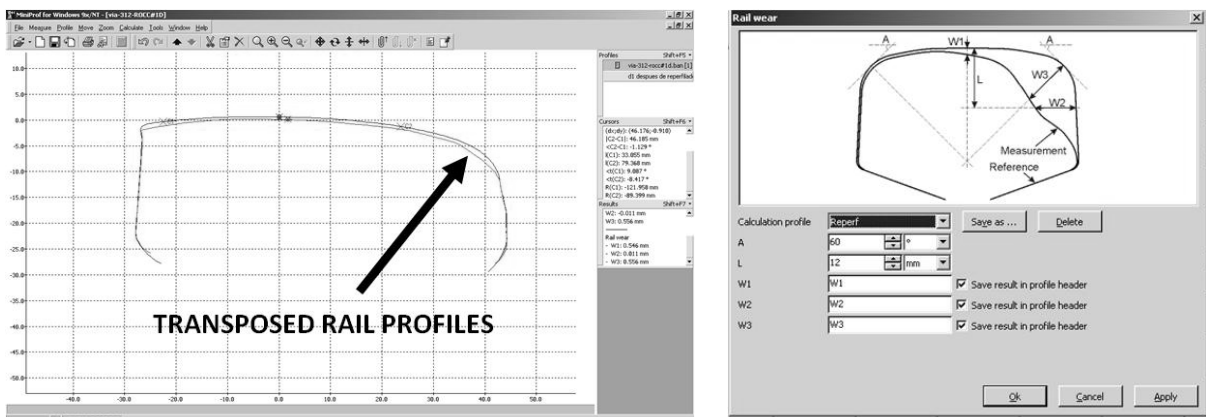
**Table 1.** Details of grinding procedures

Grinding procedure	Power/ KW *	Velocity/ Kmh <sup>-1</sup>
D1	14	3.5
D3	8	3.5
D4	14	7.5
D6	8	7.5

\* The power consumed by the hydraulic motor attached to the grinding wheels is related to the actual contact pressure applied to the rail during grinding operation

### 2.3 Measurement of rail profiles

The rail profiles were measured before and after the rail grinding tests in order to evaluate the dimensional changes. The measurements were carried out by using a *Miniprof* system and the changes in parameters W1, W2 and W3, as defined in figure 2b, were reported for each rail grinding procedure. The initial profile of the rail in every measured position was transposed with the ground profile to determine the changes in every parameter and the rails were aligned using the same criterion.



a) Example of transposing of rail profiles to calculate removed material

b) Definition of W1, W2, and W3 parameters

**Figure 2.** Measurement of rail profiles. W1 is the vertical rail head wear, W2 is the horizontal rail flange wear and W3 is an angular measurement at 45° of rail wear.

## 2.4 Roughness Measurements

The roughness of the ground rails was measured by using a stylus profilometer with tip radius of 1  $\mu\text{m}$  and resolution power of 0.01  $\mu\text{m}$  (*Mitutoyo SurfTest 3000*). A cutoff length of  $L=0.8\text{mm}$  was selected for all the measurements according to ISO 4288 standard, and the total traversing length was 4.8 mm (0.4mm pre-travel+4mm evaluation length+0.4mm post-travel). Roughness parameters  $R_a$ ,  $R_q$ ,  $R_t$ ,  $R_v$ ,  $R_{sm}$ ,  $R_k$ ,  $R_{sk}$  following ISO 4287 standard, were used to characterize the surfaces. The values correspond to the average of 6 measurements performed on the same rail zone. The selected zone was inside the contact patch for the curve from where the rails were extracted.

## 2.5 Sectioning and Metallographic Inspection

After the roughness measurements, the rail was cut, mounted and polished in order to evaluate the microstructure near the surface. The surfaces were evaluated using SEM. The microstructure was analyzed by Light Optical Microscopy (LOM) using a *Nikon Eclipse LV100* with a *Nikon Digital Sight DS-2Mv* camera and SEM. The rails were etched using Nital 2% and Picral.

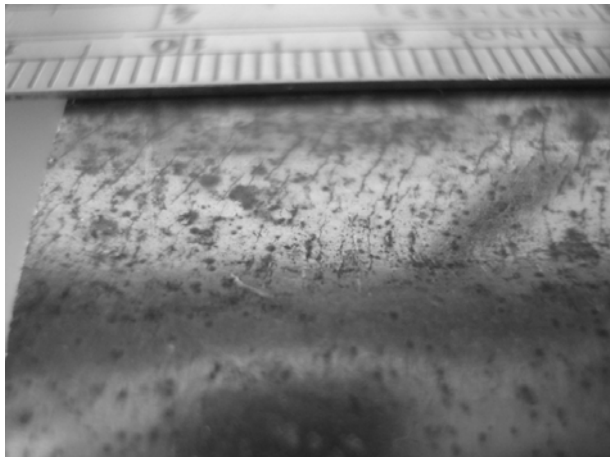
Micro-hardness measurements were carried out in the cross section of each ground specimen by using a *Shimadzu Type M* micro-hardness tester, with a resolution of 0.5  $\mu\text{m}$  according to ASTM E-384 Standard. Phases on the deformed zone near the surface were identified by X-Ray Diffraction (XRD) with the aid of a *Phillips X'Pert Pro* diffractometer with Cu K $\alpha$  radiation equipped with a 2D solid-state detector.

## 3 RESULTS AND DISCUSSION

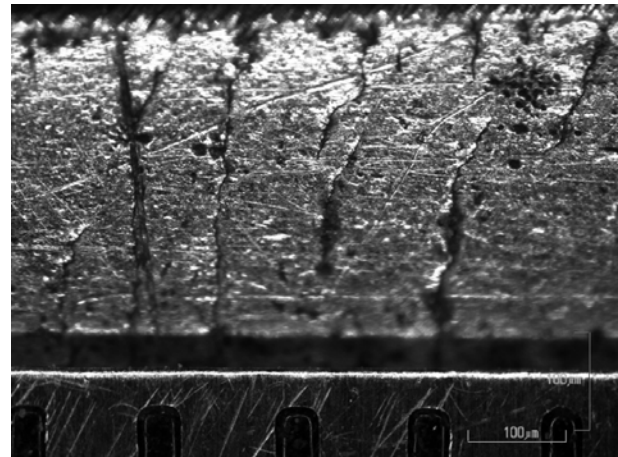
### 3.1 Inspection of Fatigued Specimens

The inspection of fatigued rails revealed the presence of parallel cracks at the surface, which are commonly reported in literature as head checks.<sup>(6)</sup> These cracks grow from inside the rails and in some cases can cause catastrophic rail failures.<sup>(7)</sup> Head checks must be removed by reprofiling and their growth rate defines the “magic” wear rate of the rail, which plays a key role in controlling wear by rail grinding.<sup>(8)</sup> In this case, the inspected rail had an average of 3 cracks per square millimeter (see Figures 3a and 3b for reference). The inspection of the cross section revealed that, on average, the crack depth was 0.5 mm (see Figures 3c and 3d). The angle between the rail surface plane and the cracks was around 35-45 degrees. Some iron oxides were found inside the cracks as a result of the interaction with the ambient. According to these findings and the operator's experience, the grinding procedures were designed to remove 0.5 mm from the surfaces.

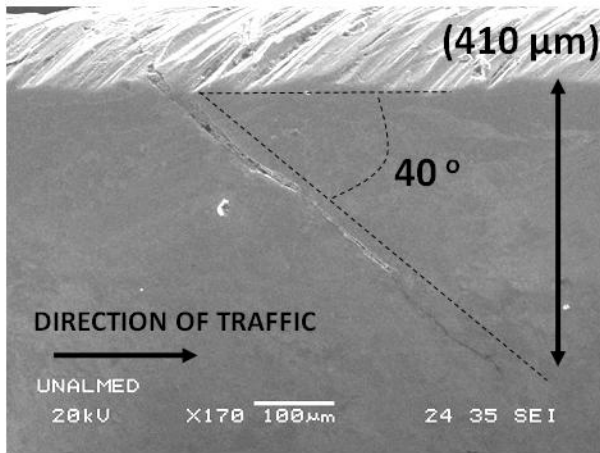




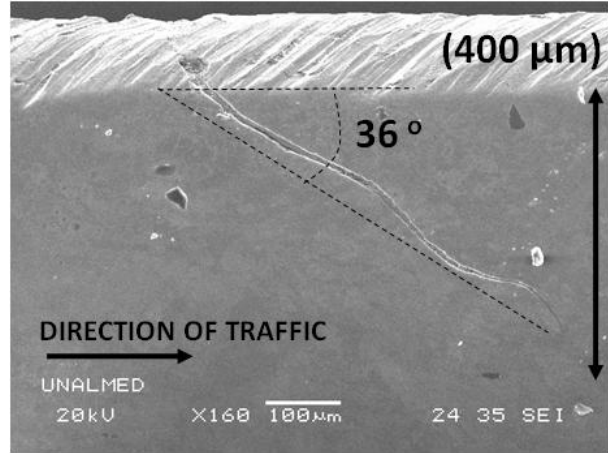
a) Head checks on the surface



b) Detail of head checks



c) Crack observed at the surface



d) Crack observed at the surface

**Figure 3.** Inspection of fatigued rails.

### 3.2 Profile Changes After Rail Grinding

Figure 4 shows the changes in W1, W2 and W3 parameters after reprofiling. It can be seen that only two procedures are effective to remove cracks and they are associated with higher pressures used during the test. W2 parameter is higher when a low pressure is applied to the rail, but its variation is not significant when compared with those of W1 and W3. Although grinding velocity plays an important role on the mass removing process, the greatest differences before and after the tests were obtained when the pressure (power) was modified and the reprofiling velocity was kept constant. This can be verified by comparing, for instance, procedure D1 (14 KW, 3.5 Kmh-1) with procedure D3 (8 KW, 3.5 Kmh-1) in Figure 4.

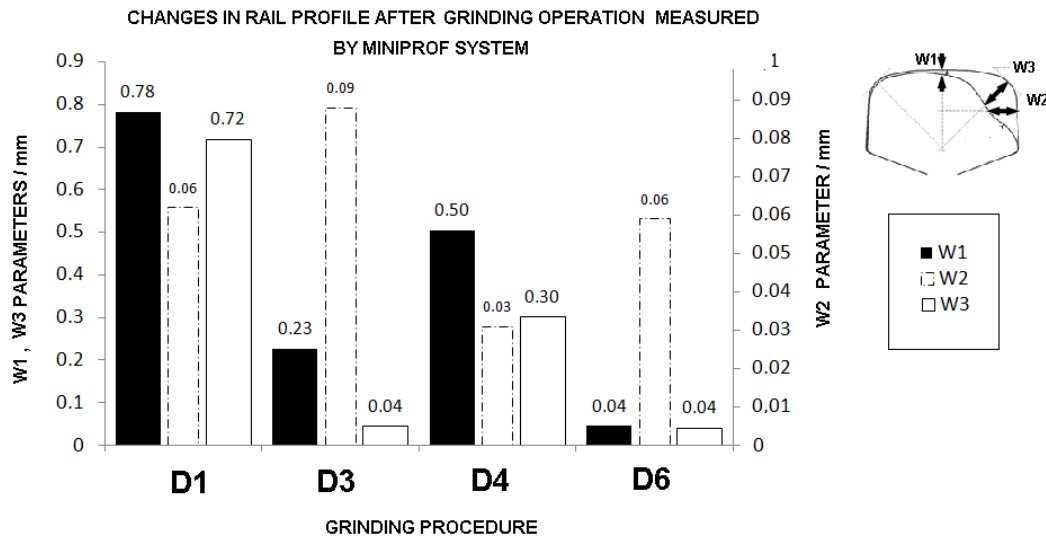


**Figure 4.** Changes in rail dimensions after grinding.

### 3.3 Roughness Variations

Figure 5 shows that the variation of pressure and velocity during grinding operation did not lead to significant differences in roughness. Additionally, the measured roughness parameters are very low compared with the values typically found in international reports ( $R_a < 10 \mu\text{m}$ ).<sup>(9)</sup> It is worth noticing, however, that the interval of permitted values according to international standards is quite wide and can lead to consider as acceptable surfaces with roughness profiles prone to localized high local pressures, which can cause accelerated fatigue of the rails. On the other hand, skewness parameters indicate that the profiles are very symmetric with respect to the reference line, which means that the probability of finding peaks and valleys is very similar along the roughness profile. Kurtosis values are near 3 (Gaussian surface) and no differences were found for different reprofiling procedures.

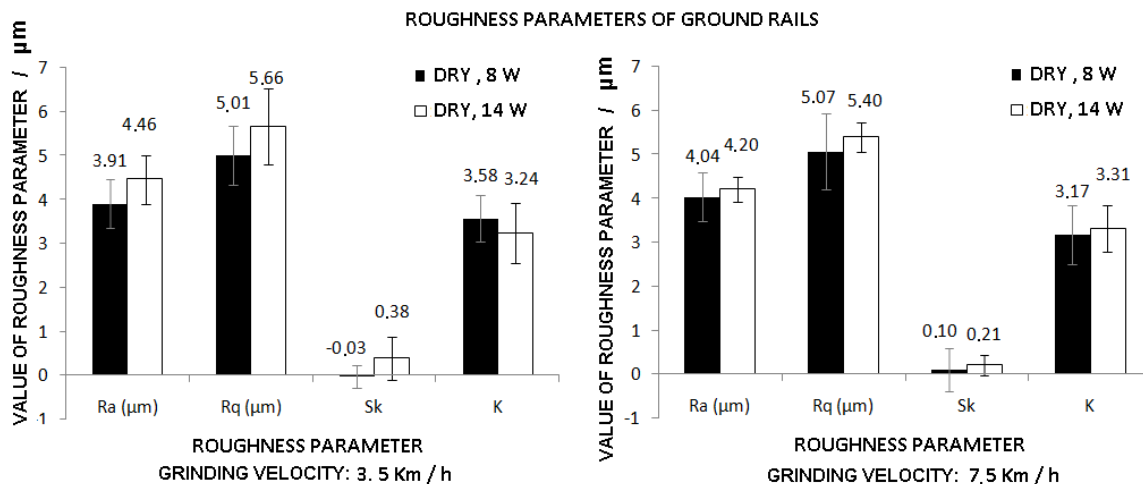


**Figure 5.** Roughness parameters of ground rails using different procedures.

Figure 6 shows the ground surfaces after D1, D3, D4 and D6 procedures. It can be seen that only D1 procedure was effective over the entire rail surface, as opposed to procedures D3, D4 and D6 that left a black zone where the wheels did not grind the rail's surface. On the other hand, the marks seen after the low velocity procedures

(D1 and D3) were clearly more uniform. According to these results, low velocity grinding is recommended for better results in terms of homogeneity of the surface.

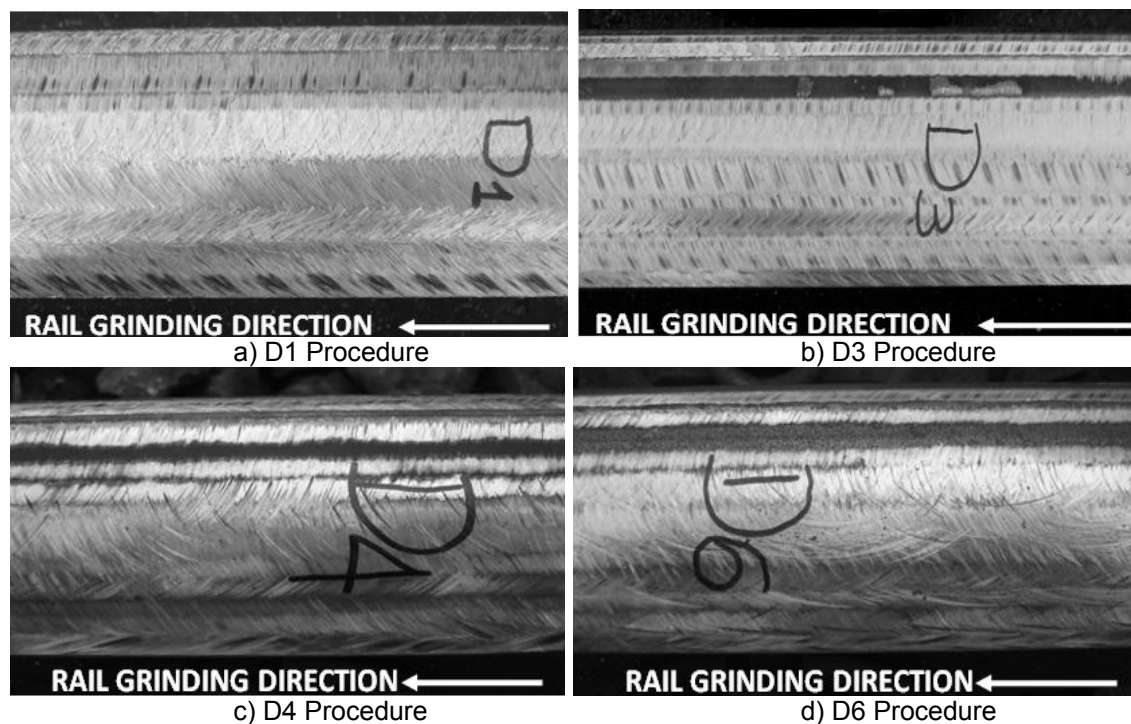


Figure 6. Aspect of rail's surface after different grinding procedures. a) D1, b) D3, c) D4, d) D6.

### 3.4 Microstructure of Ground Rails

The microstructure of the R260 rail in a zone far from the surface was composed of perlite and proeutectic ferrite with an average hardness of  $325 \pm 12$  HV (Figure 7a). When the ground surfaces were inspected, two main regions were observed: a white layer near the surface and a deformed zone beneath it.

The white layer thicknesses were 15, 15, and 10  $\mu\text{m}$  for D1, D3, and D4 procedures respectively. No white layer was observed after D6 procedure. The microstructure obtained after D6 reprofiling procedure is not discussed in detail here because such procedure was not effective to remove material from the surface of the rail. The thicknesses of the deformed layers were 400, 250 and 300 microns for D1, D3 and D4 respectively.

Further study is needed to conclude about relations between the thickness of the deformed layer and the grinding procedures, especially because the layers are not uniform as a result of the differences in pressure of the grinding wheels, as can be inferred from the analysis of profiles. Generally speaking, however, it can be said that, for a given pressure, increasing linear grinding velocity reduces the depth of the deformed layer.

The hard white layer was found in all the inspected rails and it had cracks parallel to the surface (arrow 1 in Figure 7b). Its aspect and the results of hardness measurements (see Figure 8) indicate that it is composed of untempered martensite formed due to localized heating and fast cooling during the grinding procedures, which has been previously reported by Chandrasekar et al.<sup>(10)</sup> Figure 7c shows the white layer (1) and deformed layer (2) after procedure D1 while arrow 1 in Figure 7d shows the hard layer after procedure D4.



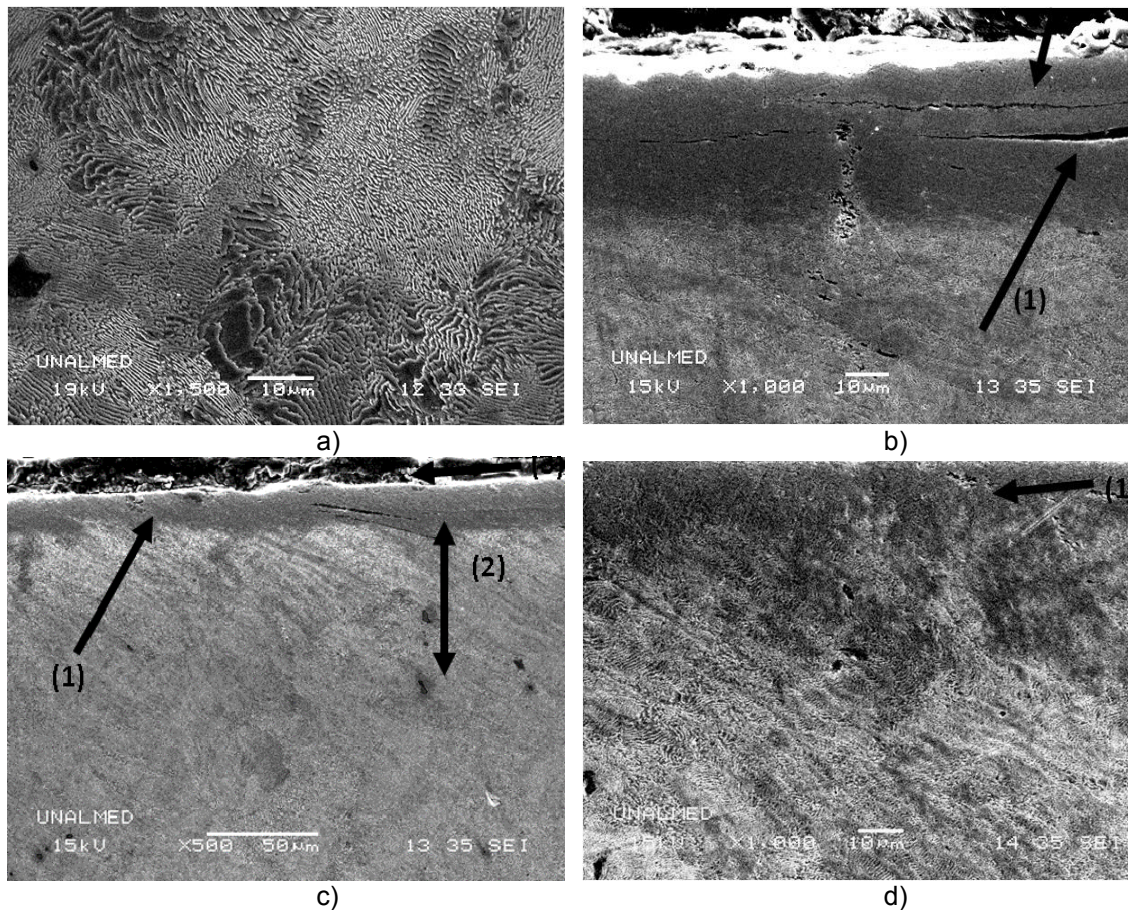


**Figure 7.** Rail microstructures for a) Undeformed rail (region far from the contact surface) showing cracks parallel to the contact surface, b) Sub-surface white layer, procedure D1, c) Sub-surface white layer (1) and deformed layer (2), D1 procedure, d) Sub-surface white layer, procedure D4.

Micro-hardness measurements performed in ground rails after procedures D1, D3 and D4 at locations of maximum susceptibility to RCF cracking on the rails are shown in Figure 8. Data were acquired in the same measurement direction of the W3 parameter analyzed in section 3.2. It can be seen that D1 procedure led to the highest hardness value at 800 µm depth, followed by D3 and D4 procedures respectively; those results are related to the effect of rail grinding pressure on the degree of strain hardening associated to this process. Further studies are required to conclude about the influence of the strain hardened layer on the RCF in ground rails and how it could be related with shakedown models proposed in the literature.<sup>(11,12)</sup>



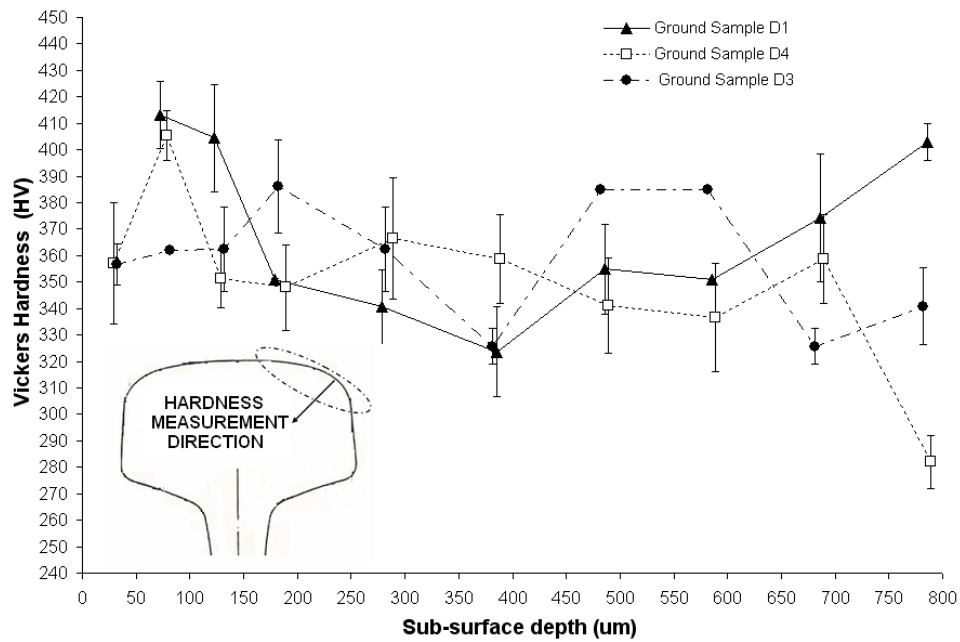
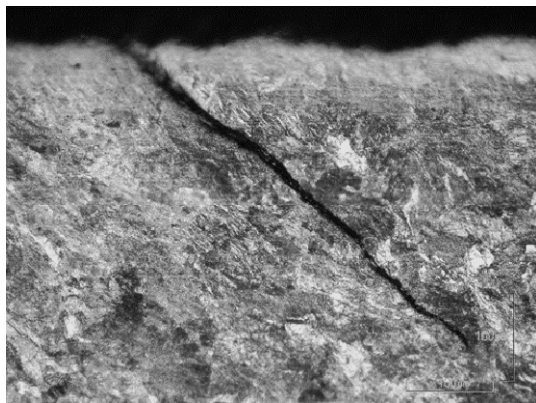
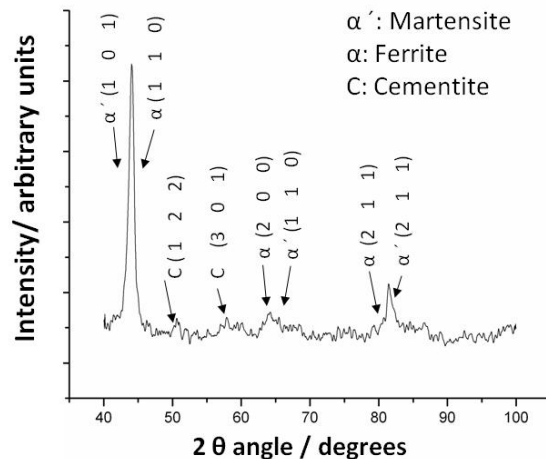


Figure 8. Micro-hardness measurements at three ground rails.

Figure 9a shows the microstructure near the surface before grinding and Figure 9b shows an XRD pattern taken from the ground surface. It can be observed that the grinding procedure effectively changes the microstructure of the subsurface since fresh martensite is formed, and consequently the fatigue response of the rails is presumably affected. In particular, micro-cracks formed at the surface as a consequence of martensitic transformation can act as nucleation sites for fatigue cracks, whose growth notably reduces the fatigue life of the rails. The formation of a hard layer during reprofiling has been recently reported by Kanematsu.<sup>(13)</sup>



a) Microstructure near the surface before the grinding tests



b) XRD pattern after the grinding tests

Figure 9. Microstructure before grinding (a) and XRD pattern of D1 ground rail (b).

#### 4 CONCLUSIONS

- Inspection of a commercial fatigued rail showed cracks parallel in the surface (head checks), which were oriented around 36-45 degrees with respect to the traffic direction and had a depth of penetration of circa 0.5 mm.

- A hard layer of martensite of circa 10-20  $\mu\text{m}$  in thickness was observed near the surface of the ground rails. This white layer can significantly reduce the resistance to rolling-contact fatigue of the rails.
- Among the studied reprofiling procedures, only the procedure performed at 3.5  $\text{Kmh}^{-1}$  and a pressure (power) of 14 W (procedure D1) was effective to grind the entire rail surface. The size of the white layer in this case was 15  $\mu\text{m}$ .

## Acknowledgements

The authors thank *Metro de Medellín* for technical support. Financial support provided by Colciencias-Metro de Medellín-UNAL, project No. 20201005975 is also acknowledged.

## REFERENCES

- 1 Kapoor, F.J. Franklin, S.K. Wong, M. Ishida, Surface roughness and plastic flow in rail wheel contact, *Wear* 253 (2002), 257–264.
- 2 F. Bucher, K. Knothe, A. Theiler, Normal and tangential contact problem of surfaces with measured roughness, *Wear* 253 (2002), 204–218.
- 3 H. Chen, M. Ishida, T. Nakahara, Analysis of adhesion under wet conditions for three-dimensional contact considering surface roughness, *Wear* 258 (2005), 1209–1216.
- 4 Koan-Sok Baek, Keiji Kyogoku, Tsunamitsu Nakahara, An experimental investigation of transient traction characteristics in rolling–sliding wheel/rail contacts under dry–wet conditions, *Wear* 263 (2007), 169–179.
- 5 Yukio Satoh, Kengo Iwafuchi, Effect of rail grinding on rolling contact fatigue in railway rail used in conventional line.
- 6 M. Takikawa, Y. Iriya, Laboratory simulations with twin-disc machine on head check, *Wear* 265 (2008), 1300–1308.
- 7 Management and Understanding of Rolling Contact Fatigue-Literature Review, Rail Safety & Standards Board Report, United Kingdom, July 2006.
- 8 J. Lundmark, “Rail Grinding and its impact on the wear of Wheels and Rails,” Licentiate Thesis, Lulea University of Technology, LULEÅ, Sweden, 2007.
- 9 Rail Grinding Standard for Plain Track ETM-01-02, Australian Rail Track Corporation, Adelaide, Australia, May 2008.
- 10 S. Chandrasekar, T.N. Farris, R.R. Hebbbar, S.A. Hucker, and V.H. Bulsara, Thermal Aspects of Surface Finishing Processes, in: *ASM HANDBOOK: Surface engineering*, Volume 5 (1994), pp 341.
- 11 Kapoor, A re-evaluation of the life to rupture of ductile metals by cyclic plastic strain, *Fatigue Fract. Eng. Mater. Struct.* 17 (2) (1994) 201–219.
- 12 Kapoor, F.J. Franklin, S.K. Wong, M. Ishida, Surface roughness and plastic flow in rail-wheel contact, *Wear* 253 (1–2) (2002) 257– 264
- 13 Y. Kanematsu, Y. Satoh, K. Iwafuchi. Influence of type of grinding stones on efficiency of rail grinding. Proceeding of the 8th International Conference on Contact Mechanics and Wear of Rail/Wheel Systems (CM2009), Firenze, Italy, September 15-18, 2009.